Magnetothermal force on heated or cooled pipe flow

MAGNETOTHERMAL FORCE ON HEATED OR COOLED PIPE FLOW

Masayuki Kaneda* and Kazuhiko Suga

Osaka Prefecture University, 1-1 Gakuencho, Naka-ku, Sakai 599-8234, Japan

ABSTRACT

The effects of the magnetothermal force on the flows of heat and fluid through a pipe are investigated numerically when the pipe wall is either heated or cooled at constant heat flux. The flow is laminar and a paramagnetic fluid is presumed as the working fluid. Because the magnetic susceptibility of a paramagnetic fluid depends on the inverse of its temperature, the magnetothermal force is induced by coupling of the temperature field and magnetic induction. First, the effects are discussed using the case of a magnetic field induced by a single-turn concentrically placed electric coil. It is found that the effects of the magnetothermal force differ according to whether the pipe is cooled or heated. When cooled, the heat and fluid flows are affected behind the coil; the flow is repelled from the wall to the center and the thermal boundary layer thickens. By decomposing the force into the radial and axial directions in the heated and cooled cases, it is clarified that the axial force changes from positive to negative depending on the coil location in the heated case. Therefore, it can be concluded that the effects are not simply oppositional in the heated and cooled cases. In relation to the heat transfer, only when the coil is placed at the threshold of the heating/cooling zone do the effects on the local heat transfer become the opposite of each other. At other coil locations, the suppression of heat transfer is dominant ahead of the coil in the heated case, as indicated in previous work by our group. However, in the cooled case, this effect occurs behind the coil. For a more practical case, a solenoid coil is employed in the simulation. It is then found that the effect on the heat transfer becomes remarkable at the solenoid edges, especially for the heat-transfer suppression in both the heated and cooled cases.

KEYWORDS: Magnetothermal force, pipe flow, heated, cooled, local heat transfer

NOMENCLATURE

B	dimensionless magnetic induction
C	constant
D	dimensionless diameter
FR	dimensionless force in radial direction
FZ	dimensionless force in axial direction
g	acceleration due to gravity, m/s^2
k	thermal conductivity of fluid, W/m^2
P	dimensionless pressure
Pr	Prandtl number
q	heat flux, W/m^2
Q	dimensionless heat flux
R	radial coordinate
Ra^*	modified Rayleigh number
T	dimensionless temperature
T_{bulk}	local mixed mean temperature
T_{wall}	local wall temperature
U	dimensionless velocity
Z	axial coordinate

*Corresponding Author: mkaneda@me.osakafu-u.ac.jp

α thermal diffusivity, m^2/s
β expansion coefficient due to temperature, 1/K
γ magnetization number
ϕ circumferential coordinate
μ viscosity, Pa s
μ_m magnetic permeability, H/m
χ mass magnetic susceptibility, Wb m/kg

HIGHLIGHTS

- Effect of the magnetothermal force differs depending on whether the pipe wall is heated or cooled.
- The magnetothermal force induced on the heated pipe wall acts like a front-loaded bump.
- For the cooled pipe wall, this force behaves like a back-loaded round cavity.
- The local heat transfer is affected correspondingly.
- The magnetic field of a solenoid coil can reduce the heat transfer rate.

1. INTRODUCTION

Magnetic susceptibility is a physical property. Materials with positive magnetic susceptibility are attracted to magnets, whereas those with negative susceptibility are repelled. Ferromagnetic materials (e.g., iron, cobalt, nickel) have large positive magnetic susceptibility ($>10^9$ cm^3/g), whereas paramagnetic materials have small positive susceptibility (e.g., oxygen: $\sim 10^{-4}$ cm^3/g). Although the magnetic force on paramagnetic materials is extremely small, its effect was detected in the 19th century [1] and has since been applied to, for example, oxygen gas sensors.

In the late 20th century, extremely strong magnetic fields became available with the emergence of superconducting magnets. Magnetic fields of several tesla or more have allowed various new findings such as the levitation of water droplets under gravity (magneto-Archimedes effect) [2], jets of nitrogen gas in air (Wakayama jet) [3], and nonmagnetic particle alignment [4]. Each of these phenomena is induced by a magnetic force on a material that is not electrically conductive, as given by

$$f = \Delta\chi \nabla B^2 / 2\mu_0 \,. \tag{1}$$

This suggests that overall force is due to differences in magnetic susceptibility among the various materials involved in each phenomenon.
Another characteristic of the magnetic susceptibility of a paramagnetic material is that it depends on the inverse of absolute temperature:

$$\chi = C/T, \tag{2}$$

where C is a constant. This is known as Curie's law. Therefore, even for a single component, a magnetic force is induced that depends on the local temperature. This is known as the magnetothermal force. In terms of problems involving the flow of heat and fluid, this force can be used to control convection, and many such studies have been reported to date. Braithwaite et al. [5] found that Rayleigh–Bénard convection is enhanced/suppressed under a strong magnetic field by placing above/below a superconducting magnet. Uetake et al. [6] demonstrated the spontaneously induced flow of air in a tube due to the combination of a heater and a superconducting magnet. Kaneda et al. [7] reported the convection of air under thermally stratified conditions in a cubic enclosure. Kenjereš et al. [8, 9] investigated oscillatory convection in a magnetic field for a paramagnetic fluid in a cubic enclosure heated from bottom and cooled from above.
Convection control is also possible in case of forced convection. Our group has implemented the magnetothermal force in a lattice Boltzmann code for heat and fluid flows, and has investigated the effect of this force on flow through a heated open-cell porous medium [10]. It was found that the magnetothermal force enhances the local heat transfer inside the porous medium.

As a simpler case, we consider heat and fluid flows through a tube. Heat transfer in a straight tube occurs in various heat exchangers, the performance of which depends on the ability to control the heat transfer. Kaneda et al. [11] considered heat-exchange tubes that are heated externally. In particular, they reported the effect of the magnetothermal force on the flow of heated paramagnetic fluid in a pipe at a constant flow rate (i.e., fixed Reynolds number). They discussed the roles of magnet location, Reynolds number, and magnetic induction. It was found that the magnetothermal force induces vortex flow in the vicinity of the magnet and that heat transfer is suppressed in front of the magnet and enhanced behind it. For pressure-driven flow inside the tube [12], the flow pattern changes and the heat-transfer enhancement is weakened compared with above case. It was suggested that the magnetothermal force increases the pressure loss by acting like a rib on the internal surface of the pipe, which eventually reduces the flow flux. Kaneda et al. [12] also implied that the effect of the magnetothermal force decreases with Reynolds number. Additionally, millimetre-scale flow or less is preferable for the application of low-cost magnets such as permanent magnets.

The aforementioned studies were focused on heat-exchange tubes that were heated by the surrounding medium. Clearly, another possible situation is where the tube and the medium flowing inside it are cooled (e.g., automotive radiators). In such a case, when the magnetothermal force is applied to the cooled fluid, its effect is not symmetric to that in the heated case. This is because magnetic susceptibility is proportional to the inverse of the absolute temperature, as indicated in Eq. (1). In other words, the magnitude of the force is not the same because of the above mechanism. Little attention has been given to the difference in magnetothermal force between heated and cooled cases in the presence of a main flow.

In this study, three-dimensional finite difference computations are performed to investigate the effect of the magnetothermal force on pressure-driven flow in a pipe whose wall is either heated or cooled at constant heat flux. Because this study is focused on flow inside a small tube bundled in micro heat exchangers, the acceleration due to gravity is neglected.

2. SCHEMATIC MODEL AND GOVERNING EQUATIONS

A schematic of the computational problem is shown in Fig. 1. A straight pipe with a dimensionless radius of 1.0 and length of 10 is either heated or cooled at constant heat flux at $Z \geq 1.0$. A paramagnetic fluid is driven by a given pressure difference between the inlet and the outlet of the pipe. The inlet fluid temperature is $T = 0.0$ and a free-outflow condition is employed at the outlet. The working fluid is incompressible and Newtonian, and thermal dissipation is neglected. In this study, the effect of the magnetothermal force on heated or cooled situations is investigated. To focus solely on this effect, buoyancy is neglected. As such, the cases considered in this study are applicable to microgravity situations.

In the present study, two types of magnetic field are targeted. One is that of a coaxial single-turn electric coil of radius 1.1 placed arbitrarily at *Zc* as in Fig. 1(a) for simplicity when discussing the difference between heated and cooled cases. The induced magnetic field becomes toroidal. The other is that of a 10-turn solenoid coil as shown in Fig. 1(b) for a more practical situation.

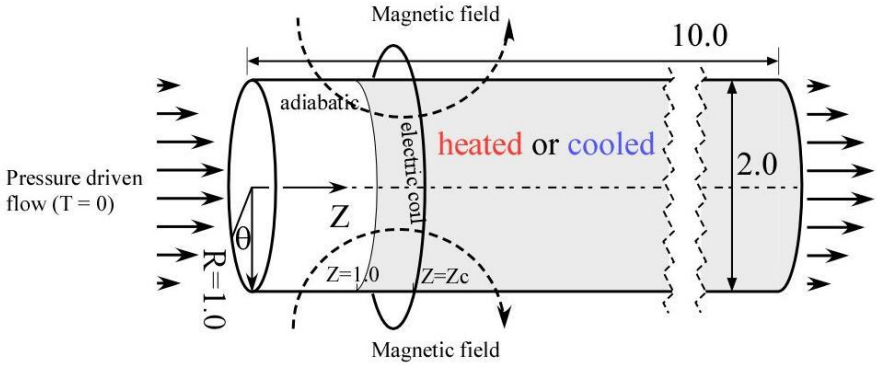

(a) One-turn electric coil

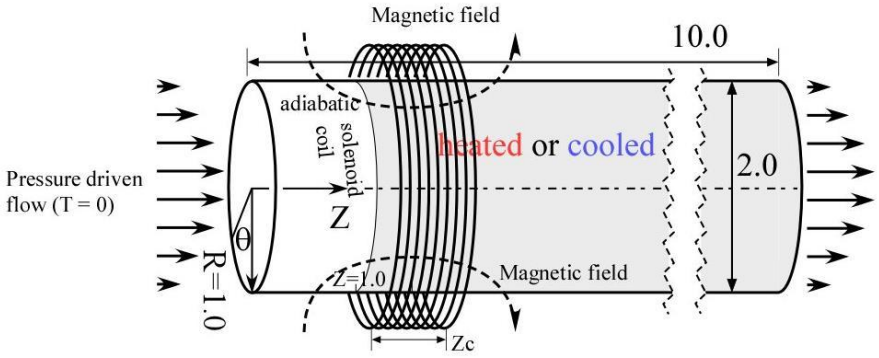

(b) 10-turn solenoid coil

Fig. 1. Schematic of computational model.

The dimensionless governing equations consist of conservations of continuity, momentum, and thermal energy. The Biot–Savart law is used to compute the magnetic field at the first time step of the computation. In the present study, a pipe of small diameter is presumed, thus buoyancy is neglected and only the magnetothermal force is considered as an external force in the momentum equation:

$$\nabla \cdot \boldsymbol{U} = 0, \tag{1}$$

$$D\boldsymbol{U}/D\tau = -\vec{\nabla}P + \mathrm{Pr}\nabla^2\boldsymbol{U} - Ra^* \mathrm{Pr} T \gamma C \vec{\nabla} B^2/2, \tag{2}$$

$$DT/D\tau = \nabla^2 T, \tag{3}$$

$$\boldsymbol{B} = -\frac{1}{4\pi}\oint \frac{\boldsymbol{R}\times d\boldsymbol{S}}{R^3}, \tag{4}$$

where

$$\mathrm{Pr} = \nu/\alpha,\ Ra^* = g\beta\dot{q}\ell^4/\alpha\lambda\nu,\ \gamma = \chi b_0^2/\mu_m g r_0,\ C = 1 + 1/\beta\theta_0\ .$$

The dimensionless parameter γ represents the magnitude of the magnetic induction. The heat flux from the pipe wall is defined by the modified Rayleigh number Ra^*. The coefficient C is used in formulating the magnetothermal force to facilitate volumetric expansion to the mass magnetic susceptibility [9].
These equations are discretized in three-dimensional cylindrical coordinates. The governing equations are solved by a finite difference scheme on staggered grids. The numbers of grids are (R, θ, Z) = (21, 24, 201) and a uniform grid system is employed except in the radial component, for which the grid size becomes finer near the wall as shown in Fig. 2. Because the targeted flow regime is laminar, this grid refinement is sufficient. The third-order upwind scheme is used for the inertial terms, the second-order central difference scheme is used for the diffusion terms, and the time marching is solved by the first-order explicit scheme. The pressure–velocity correction is solved using the HSMAC method of Hirt et al. [13]. The velocity at the axis of the three-dimensional cylindrical coordinates is treated using the method of Ozoe and Toh [14]. The profiles of induced magnetic field and resulting ∇B^2 component are identical to those of Kaneda et al. [11].

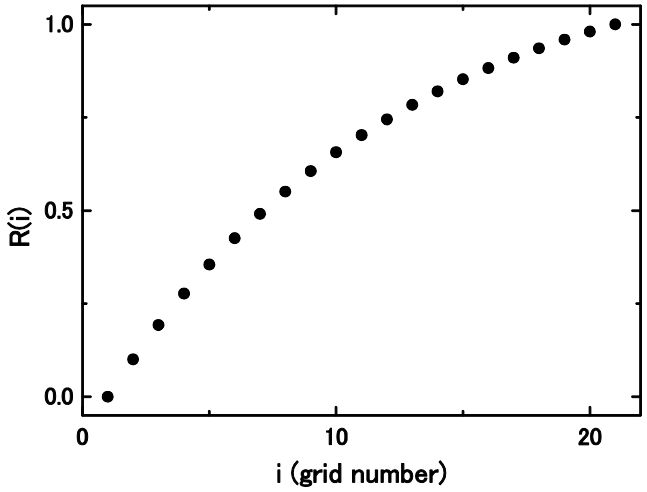

Fig. 2. Control-volume coordinate in radial direction.

The pipe wall is either heated or cooled at constant heat flux:

$$R\left.\frac{\partial T}{\partial r}\right|_{R=1.0,\,Z\geq 1.0} = \begin{cases} +1.0 & (\text{heated}) \\ -1.0 & (\text{cooled}) \end{cases} \tag{5}$$

The flow is driven by pressure boundary conditions at the pipe inlet and outlet, namely

$$P\big|_{Z=0} = +\Delta P/2, \quad P\big|_{Z=10} = -\Delta P/2\,. \tag{6}$$

The initial conditions are as follows. The fluid is stationary and the temperature is zero. The pressure is distributed linearly from inlet to outlet for faster convergence in the early stage of the computation.
In this study, ΔP is set at 2.0×10^5–1.0×10^6. The range of resulting Reynolds number without magnetic field is 12.5–62.4. The dimensionless magnetic induction γ ranges from zero (no magnetic field) to 0.5.
The working fluid in this study is an aqueous solution of gadolinium nitrate. This is a representative paramagnetic fluid on which many studies have been performed both numerically and experimentally [5, 8, 9, 12, 13]. The physical properties used in this study come from Ref. [9], and certain key ones are listed in Table 1.

Table 1. Physical properties of 0.8-mol/L $Gd(NO_3)_3$, $6H_2O$ at 298 K [9]

Thermal diffusivity, α	7.16×10^{-8}	m^2/s
Expansion coefficient due to temperature, β	4.78×10^{-4}	1/K
Thermal conductivity, λ	0.519	W/mK
Kinematic viscosity, ν	1.43×10^{-6}	m^2/s
Density, ρ	1348	kg/m^3
Mass magnetic susceptibility, χ	2.32×10^{-7}	m^3/kg

The nondimensional computational parameters can be calculated as Prandtle number $Pr = \nu/\alpha = 20.0$ and $C = 8.02$. Note that the value of C that was employed was that of the solvent (water) in Ref. [15]; this was done because of a lack of data regarding the density of the solution. This suggests that the effect of the magnetothermal force in Ref. [15] might have been overestimated. The flux of heat to/from the pipe wall is represented by Ra^*, which is fixed at 10^4. For reference, the dimensional values corresponding to above nondimensional parameters of $Ra^* = 10^4$ and $\gamma = 2.0$ for gadolinium aqueous solution [9] are as follows. When the inner diameter of the pipe is taken as 5 mm, the heat flux is 180 W/m^2 and the strongest magnetic induction

in the computational domain is 0.77 T. The Reynolds number becomes 31.2 at $\Delta P = 5.0\times10^5$. In the case, the flow rate is 1.75×10^{-7} m^3/s.

3. RESULTS AND DISCUSSION

3.1. Heat and Fluid Flows

In this subsection, we have been presuming the magnetic field to be that of the one-turn coil. The resulting magnetothermal force, streamlines, and isothermal contours are shown in Fig. 3 for both the heated and cooled cases at $\gamma Ra^* = 0.5\times10^4$ and $Zc = 3.0$. As shown in Fig. 3(a), the magnetothermal force acts in opposite directions in the heated and cooled cases. This is because the magnetic force at $T = 0$ is defined 0. Thus the force is a repelling force from the coil at $T > 0$ (heated case) and an attracting force at $T < 0$ (cooled case). The color in the figure indicates the magnitude of the axial force component Fz and shows the same induced magnitude in the heated and cooled cases. For both cases, as the governing equations suggest, the magnitude of Fz should be related to the local temperature shown in Fig. 3(b), which is discussed later.

The heat and fluid flows are also affected by this magnetothermal force. The results are shown in Fig. 3(b). In the heated case (left-hand column), the streamlines near the pipe wall are slightly bent in front of the coil by the force directed toward the central axis, as shown in Fig. 3(a). Once downstream of the coil, the streamlines return to their original radial positions. The thermal boundary layer thickens in front of the coil because of the force, but it thins out again downstream of the coil.

In the cooled case (right-hand column), the resulting phenomena are opposite to those in the heated case. The fluid flow is fluctuated behind the coil, where the thermal boundary layer thickens. This is apparently because the magnetothermal force is directed outward from the pipe, especially near the pipe wall at the coil location (right-hand column in Fig. 2(a)). It is interesting that the flow is attracted to the pipe wall in front of the coil, as the streamlines suggest, but then it avoids the area of strong magnetic field behind the coil.

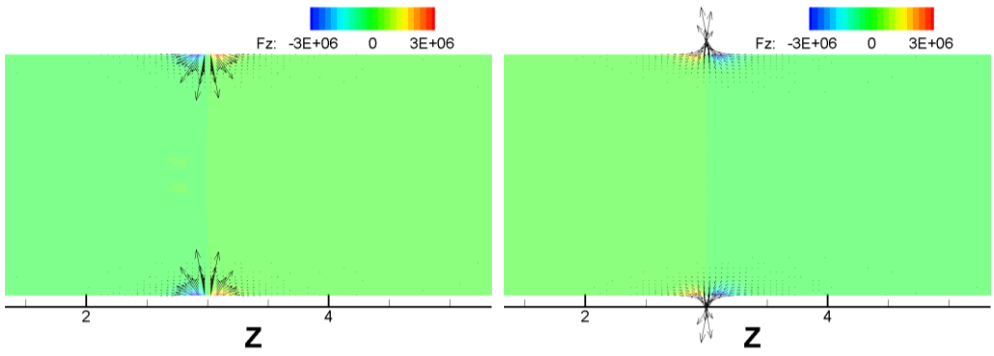

Heated case Cooled case

(a) Magnetothermal force vectors (arrows) and axial-component contours (colors).

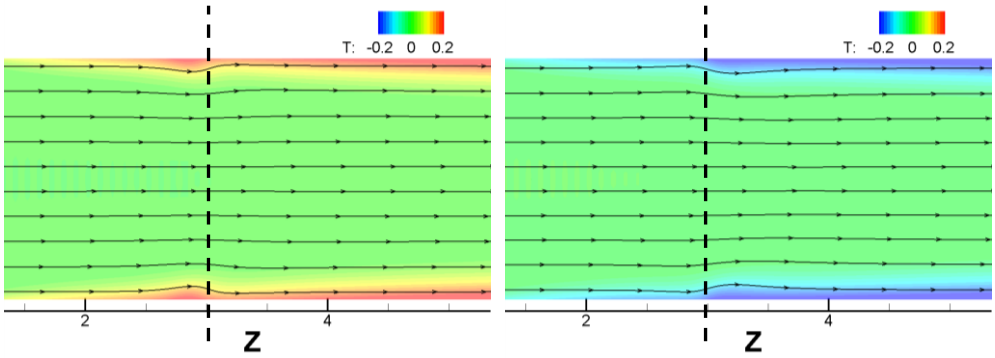

Heated case Cooled case

(b) Streamlines (arrowed lines) and isothermal contours (colors). Dashed line corresponds to coil location.

Fig. 3. Effects of magnetothermal force on heat and fluid flows at Pr = 20, $\Delta P = 5\times10^5$ (Re_0 = 31.2), $Ra^*=10^4$, and γ = 0.5. Dashed line corresponds to coil location (Zc = 3.0).

3.2. Magnetothermal Force

The magnetothermal force depends on the local temperature and the gradient of the squared magnetic induction, as the last term of Eq. (2) suggests. Because the heat flux is a given constant in this study, the local wall temperature increases with distance downstream. That is, the magnitude of the force depends on the coil location. In this section, the magnetothermal force is further discussed by decomposing it into its radial and axial components at the same computational parameters as those of Fig. 3. The radial and axial forces are given as *FR* and *FZ* in Fig. 4(a) and (b), respectively, and are defined as follows:

$$FR = \frac{\iiint F_R dR d\theta dZ}{\iiint dR d\theta dZ}, \; FZ = \frac{\iiint F_Z dR d\theta dZ}{\iiint dR d\theta dZ}, \tag{6, 7}$$

where F_R and F_Z are the radial and axial forces, respectively, at each computational cell.

At Zc = 0.5, both *FR* and *FZ* are quite weak because the coil is away from the heated/cooled zone ($Z \geq 1.0$). As shown in Fig. 4(a), as the coil is moved downstream, *FR* decreases monotonically in the heated case but increases in the cooled case. As shown in Fig. 3(a), *FR* is directed toward the central axis of the pipe (negative radial direction) in the heated case but away from it in the cooled case. The magnitudes in both cases increase as the coil is moved downstream because the deviation of the temperature from that at the inlet becomes large. For the same value of Zc, the absolute magnitudes of the forces in the heated and cooled cases are almost same. This suggests that, considering Fig. 3, the deviation in absolute temperature ahead of/behind the coil is almost symmetrical between the heated and cooled cases.

As shown in Fig. 4(b), the axial force *FZ* has a different tendency according to whether the pipe is heated or cooled. *FZ* is directed in opposite directions ahead of and behind the coil, as shown in Fig. 3(a). Note that, as defined, *FZ* is the net force in the axial direction. In the cooled case, as the coil is moved farther downstream (large Zc), the negative *FZ* value increases initially and then levels off. Because the magnetothermal force is the product of local temperature and magnetic gradient, the force becomes stronger behind the coil than in front because of the thickened thermal boundary layer as shown in Fig. 3(b). Therefore, negative values of *FZ* arise. As for the convergence of *FZ* to a constant magnitude at large Zc, this implies that the difference between the positive axial force and negative axial force becomes constant. Because the force is multiplication of the temperature and magnetic field, it can be said that the similarity of the temperature profile between ahead of and behind the coil is developed. In the case of a heated wall, *FZ* has a positive peak value at Zc = 1.0, which is the threshold of the heated region. As the coil is moved downstream, the net force changes gradually to one that is negative. It then levels off at a negative constant value as the coil is moved farther from the inlet. As suggested by Fig. 3(a) and (b), *FZ* for the heated case is in the negative axial direction and acts over a larger area in front of the coil and is in the positive axial direction and acts over a smaller area behind the coil. If Zc = 1.0, the force only behind the coil becomes remarkable, resulting in a positive *FZ* value. As the coil is moved downstream, the negative *FZ* value gradually dominates. As shown in Fig. 3(b), the thermal boundary layer ahead of the coil becomes thicker than that behind it. Thus negative *FZ* results at $Zc > 2.0$ and the levels off because of the development of the temperature field.

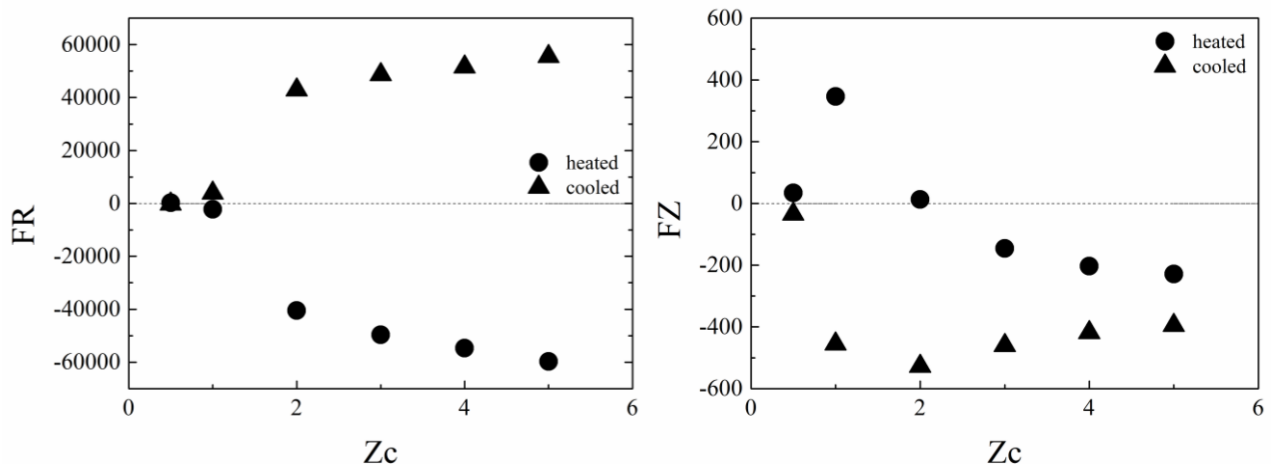

(a) Radial direction (b) Axial direction

Fig. 4. Net radial and axial components of magnetothermal force at Pr = 20, $\Delta P = 5\times10^5$ (Re_0 = 31.2), $Ra^*=10^4$, and $\gamma = 0.5$.

Considering the distribution of the magnetothermal force in Fig. 3(a), the temperature profile in Fig. 3(b), and the decomposed net forces in Fig. 4, the effect of the magnetothermal force can be understood as follows. In the heated case, it acts like a backward-facing step on the inner perimeter of the pipe at Zc = 1.0. When Zc > 1.0, the force acts like a narrow bump. According to Fig. 3, the bump is front-loaded shape. The height of the bump levels off as the coil moves farther from the heating inlet. In the cooled case, the force induces a vena contracta at Zc = 1.0. At other coil locations, it works like a back-loaded round cavity on the inner perimeter. Schematics of these two flows are shown in Fig. 5.

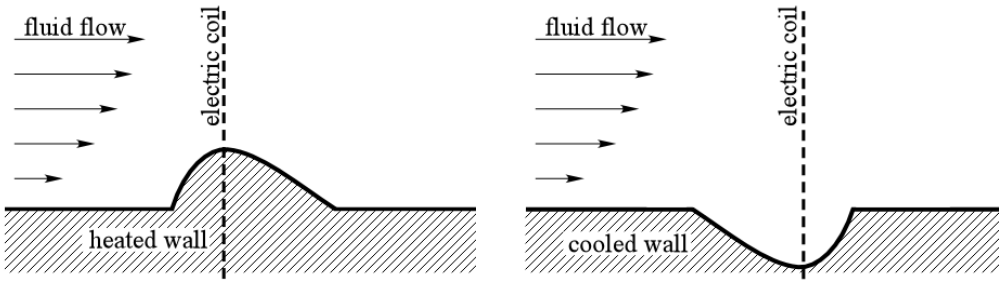

(a) Heated case (b) Cooled case

Fig. 5. Illustrations of the effects of the magnetothermal force.

3.3. Effect on Nusselt Number

The direction and magnitude of the induced magnetothermal force depend on the coil location and whether the pipe is heated or cooled. The force affects the local heat transfer from the pipe to the fluid. The effect on the heat transfer is evaluated by the locally averaged Nusselt number along the pipe wall, defined as follows:

$$Nu_{local} = \frac{QD}{(T_{wall} - T_{bulk})}, \tag{5}$$

where Q is the dimensionless heat flux (= 1.0), D is the diameter of the pipe (= 2.0), and T_{wall} and T_{bulk} are the locally averaged wall temperature and local mixed mean temperature, respectively. The results are shown in Fig. 6 and correspond to cases shown in Figs. 3 and 4.

For Zc = 1.0, the Nusselt number levels up in the heated case and levels down in the cooled case near the coil. The coil location coincides with the inlet of the heated/cooled zone. As mentioned above, the magnetothermal force acts like the backward-facing step in the heated case and as a vena contracta in the cooled case.

For other coil locations, the difference between the heated and cooled cases becomes remarkable. For example, for Zc = 3.0 in the heated case, the Nusselt number (red solid line) decreases in front of the coil and increases behind it. In contrast, the blue solid line (cooled case) behaves oppositely. These also correspond to the effect of the bump in the heated case and the cavity in the cooled case.

It is interesting that the effect on the local Nusselt number is remarkable in front of the coil in the heated case but behind the coil in the cooled case. In the heated case, a thermally stagnant region is induced in front of the coil. The Nusselt number recovers its value in the absence of a magnetic field a short way behind the coil. However, the increase downstream is small like an overshoot. In the cooled case, because the fluid is attracted toward the coil, the Nusselt number increases in front of the coil. Behind the coil, the thermal boundary layer becomes locally thick. This also attracts the fluid to the coil more strongly than is the case in front of the coil, resulting in the region of locally low Nusselt number. This behavior also corresponds to characteristics of the magnetothermal force such as the front-loaded bump in the heated case and the back-loaded cavity in the cooled case.

We note that the flow flux corresponds to the heat transfer characteristics. However, the effect on the flow flux is quite small compared with that on the local heat transfer. This is due to the small axial force compared to the radial force, as discussed in Fig. 4.

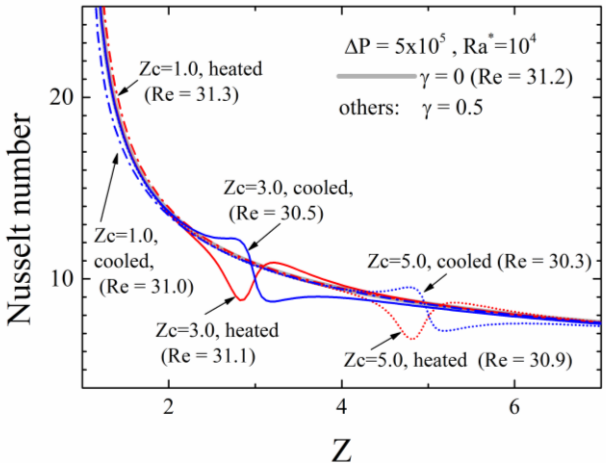

Fig. 6. Local Nusselt number along the pipe for $\Delta P = 5\times10^5$ and $Ra^*=10^4$. Red lines indicate the heated case, and blue ones indicate the cooled case.

The effect of the magnetothermal force on Nusselt number depends on the local temperature and the gradient of magnetic induction. In forced convection, it is also affected by the bulk velocity. Figure 7 shows cases at higher pressure differences in the pipe for different magnetic inductions. The Reynolds number without a magnetic field is 62.4. As the pressure difference between the inlet and outlet of the pipe increases, so does the bulk flow. In that case, the effect on the local Nusselt number becomes small, as shown in Fig. 7(a). When γ is doubled, the magnetothermal force becomes effective similarly to that in Fig. 6. The fundamental effects of the magnetothermal force on the heat and fluid flows are same. Therefore, the aforementioned bump and round-cavity effects depend on the pressure difference in the pipe, the magnetic induction, and of course the heat flux from the wall (Ra^*).

We note that the flow becomes unstable when γ is increased further. This is because, as shown in Fig. 3(a), the direction of the axial force changes suddenly at the coil location, which induces unsteady flow at high magnetic induction.

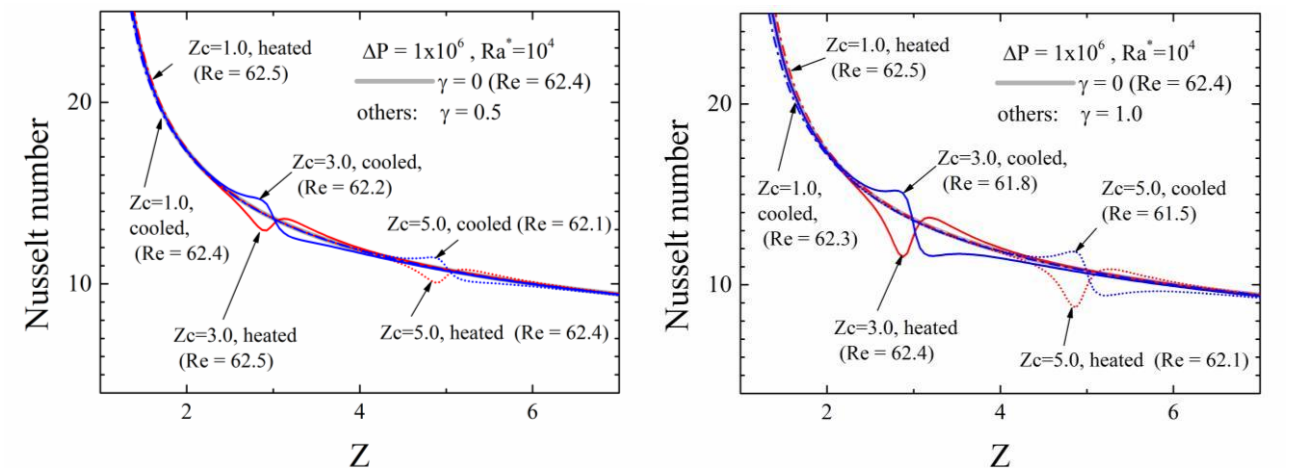

(a) γ = 0.5 (b) γ = 1.0

Fig. 7. Local Nusselt number along the pipe for $\Delta P = 10^6$ and $Ra^*=10^4$.

3.4. Solenoid Coil

In the previous sections, the difference between the heated-wall and cooled-wall cases was discussed using the magnetic field from the single-turn electric coil. We clarified that different directions of the magnetothermal force induce different characteristics of the heat and fluid flows. It should be noted that because the magnetothermal force direction changes drastically across the single electric coil, the characteristics ahead of and behind the coil are close. To represent a more practical case, a solenoid coil is employed in the magnetic field calculation. A 10-turn solenoid coil of length of 1.0 (Fig. 1(b)) is presumed in this section.

The distributions of magnetic field and ∇B^2 are shown in Fig. 8. The solenoid is located at $3.0 \le Zc \le 4.0$. This figure corresponds to the case studied by Kaneda et al. [12]. We confirm that the pitch of the solenoid is small enough to induce smooth magnetic field lines. Because the solenoid is relatively short in length, the magnetic field has a distribution inside the solenoid. The ∇B^2 distribution indicates maxima at the inlet and outlet of the solenoid.

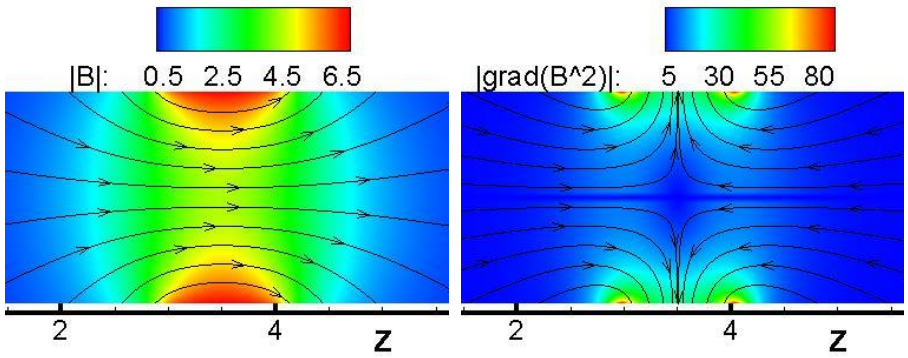

(a) Magnetic field (b) ∇B^2

Fig. 8. Distributions of magnetic field and ∇B^2 for a 10-turn solenoid coil ($3.0 \le Zc \le 4.0$).

The computed parameters related to the physical properties and heat flux from the pipe wall are the same as those in the aforementioned computations, namely $Pr = 20$, $C = 8.02$, and $Ra^* = 10^4$. The pressure difference between the inlet and outlet of the pipe is set at 10^6 ($Re_0 = 62.4$), which is identical to the case shown in Fig. 7. Because the dimensionless magnetic induction γ was defined for the one-turn coil, the dimensional magnetic induction becomes much stronger for the solenoid when the same value of γ is employed. Thus, the value of γ is reduced to 0.01 for stable computation.

The magnetothermal force, temperature field, and streamlines are shown in Fig. 9 for the heated and cooled cases. We find that the magnetothermal force becomes large on both sides of the solenoid. In particular, it is remarkable at the solenoid inlet in the heated case and at the solenoid outlet in the cooled case. The magnitude of

the force is related to the thickness of the local thermal boundary layer, as shown in Fig. 9(b). The streamlines are thus fluctuated at the inlet of the solenoid in the heated case and at the outlet of the solenoid in the cooled case.

The results can be interpreted as follows. In the heated case, the bump effect is remarkable in front of the solenoid coil. This is because the gradient of B^2 is large there and the drag force becomes effective at the solenoid inlet. Inside the solenoid, the force is directed toward the central axis but the magnitude of the force is weaker than that in front of the coil. At the solenoid outlet, even though the force is weaker than that at inlet, the force includes a positive axial component. In the cooled case, the attractive force toward the pipe wall is weak at the solenoid inlet. In contrast, the force becomes quite large near the solenoid outlet. It is directed partially in the upstream direction and so retards the flow and induces a weak vortex near the wall (not shown in the figure).

The effect on the local heat transfer is shown in Fig. 10. When the tail edge of the solenoid corresponds to the heating/cooling threshold (Zc = 0.0–1.0), the effect on the heat transfer is negligibly small in both the heated and cooled cases. This is because the magnetic induction at the solenoid inlet is small compared with the case of the single coil. If the leading edge of the solenoid coincides with the threshold and the tail edge reaches sufficiently into the heated/cooled area (Zc = 1.0–2.0), the effect of the leading edge is small (as in the Zc = 0.0–1.0 case) but the effect near the tail edge becomes remarkable; the Nusselt number is increased in the heated case and decreased in the cooled case. The force applied in this case is partially similar to that behind the center length of the solenoid of Fig. 9(a).

When the solenoid area is included in the heated/cooled region (Zc = 3.0–4.0), the magnetothermal force is of course remarkable at both the inlet and outlet of the solenoid. As mentioned above, the magnetothermal force is strong in front of the solenoid in the heated case and at the outlet of the solenoid in the cooled case, as shown in Fig. 10. Because of the length of the solenoid, the tendency of the Nusselt number plot is expanded from that in the one-turn-coil data.

Comparing the heated and cooled cases, it is apparent that the magnetothermal force is more effective in the cooled case, which is also supported by the resulting Reynolds numbers indicated in Fig. 10. This is because the effective area (i.e., tail edge of the solenoid, high ∇B^2) is far from the threshold of the cooled region in the cooled case, where the large temperature difference from the inlet is attained, which results in a stronger magnetothermal force at the outlet of the solenoid.

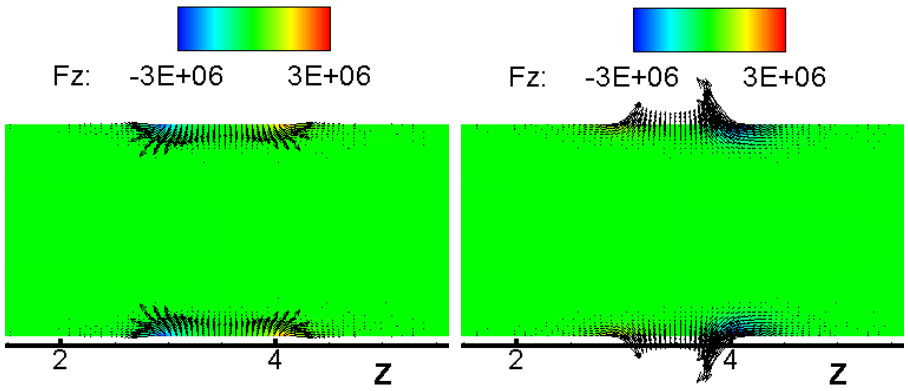

(a) Magnetothermal force

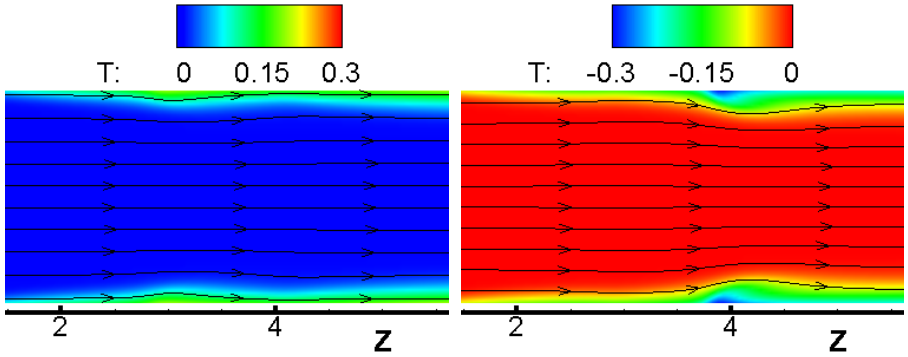

(b) Temperature and streamlines

Fig. 9. Effects of magnetothermal force induced by solenoid coil on heat and fluid flows for Pr=20, ΔP=10^6 (Re_0 = 62.4), Ra*=10^4, and γ = 0.01. The solenoid is placed at 3.0 ≤ Zc ≤ 4.0.

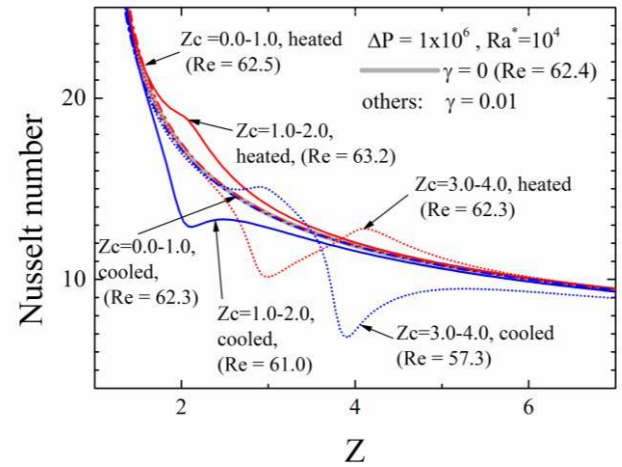

Fig. 10. Effects on local Nusselt number on the heated/cooled wall by solenoid coil for Pr=20, ΔP=10^6 (Re_0 = 62.4), Ra*=10^4, and γ = 0.01.

4. CONCLUSIONS

The effects of a magnetothermal force on the heat and fluid flows of a paramagnetic fluid (liquid) in a pipe are investigated numerically, especially the difference between cooling the pipe and heating it. In the heated case, the magnetothermal force blocks the fluid flow in front of the coil, thus suppressing the local heat transfer. The heat transfer is enhanced behind the magnet but the effect is small. From the distribution of the magnetothermal force around the coil, it can be concluded that the magnetothermal force in the heated case acts like a front-loaded bump mounted on the inner perimeter of the pipe. When the pipe wall is cooled, the heat transfer is enhanced slightly in front of the coil and suppressed behind it. This can be interpreted as a back-loaded round cavity at the inner perimeter. Because the magnetothermal force acts over a larger area at larger temperature deviations from the reference temperature, the above effect on the heat transfer becomes remarkable when the coil is placed farther downstream around the pipe within the thermally developing region. The magnitude of the force levels off in the developed region. When a solenoid coil is employed for the magnetic field, the effect on the heat transfer becomes remarkable at either end of the solenoid, especially at the tail edge in the cooled case. Comparing the heated and cooled cases, the reduction in the Nusselt number becomes more pronounced in the cooled-wall case. These phenomena have the potential for controlling the heat transfer at an arbitrary location by using a magnetic field. This could be applied to microscale heat-transfer control of a paramagnetic fluid by using strong permanent magnets.

ACKNOWLEDGMENTS

This study is partially supported by a MEXT (Ministry of Education, Culture, Sports, Science and Technology) Grant-in-aid for Scientific Research (C) [grant number 15K05838]. We thank the Edanz Group (www.edanzediting.com/ac) for editing a draft of this manuscript.

REFERENCES

[1] Faraday, M., "On the Diamagnetic Conditions of Flame and Gases," *The London, Edinburgh, and Dublin Philosophical Magazine and Journal of Science*, XXXI, third ser., pp. 401-421, (1847).
[2] Ikezoe, Y., Hirota, N., Nakagawa, J., Kitazawa, K., "Making Water Levitate," *Nature*, 393, pp. 749-750, (1998).
[3] Wakayama, N.I., "Behavior of Gas Flow under Gradient Magnetic Fields," *J. Appl. Phys.*, 69, 2734, (1991).
[4] Sun, Z., Guo, M., Vleugels, J., Van der Biest, O., Blanpain, B., "Strong Magnetic Field-Induced Segregation and Alignment of Nonmagnetic Particles," *J. Appl. Phys.*, 109, 07E301 (2011).
[5] Braithwaite, D., Beaugnon, E., Tourniew, R., "Magnetically Controlled Convection in a Paramagnetic Fluid," *Nature*, 354(14), pp. 134-136, (1991).
[6] Uetake, H., Nakagawa, J., Hirota, N., Kitazawa, K., "Nonmechanical Magnetothermal Wind Blower by a Superconducting Magnet," *J. Appl. Phys.*, 85(8), pp. 5735-5737, (1999).
[7] Kaneda, M., Tagawa, T., Ozoe, H., "Convection Induced by a Cusp-Shaped Magnetic Field for Air in a Cube Heated from Above and Cooled From Below," *J. Heat Transfer*, 124, pp. 17-25 (2002).
[8] Kenjereš, S., Pyrda, L., Wrobel, W., Fornalik-Wajs, E., Szmyd, J.S., "Oscillatory States in Thermal Convection of a Paramagnetic Fluid in a Cubical Enclosure Subjected to a Magnetic Field Gradient," *Phys. Rev. E.*, 85, 046312, (2012).
[9] Kenjereš, S., Pyrda, L., Fornalik-Wajs, E., Szmyd, J.S., "Numerical and Experimental Study of Rayleigh-Benard-Kelvin Convection," *Flow, Turbulence Combust.*, 92, pp. 371-393, (2014).
[10] Kaneda, M., Kano, H., Suga, K., "Development of Magneto-Thermal Lattice Boltzmann Heat and Fluid Flow Simulation", *Heat and Mass Transfer*, 51, pp. 1263-1275, (2015).
[11] Kaneda, M., Tsuji, A., Ooka, H., Suga, K., "Heat Transfer Enhancement by External Magnetic Field for Paramagnetic Laminar Pipe Flow," *Int. J. Heat Mass Trans.*, 90, pp. 388-395, (2015).
[12] Kaneda, M., Tsuji, A., Suga, K., "Effect of magnetothermal force on heat and fluid flow of paramagnetic liquid flow inside a pipe", Applied Thermal Engineering, Vol. 115, pp. 1298-1305, 2017.
[13] Hirt C. W., Nichols B. D., Romero N. C., "A Numerical Solution Algorithm for Transient Fluid Flows," *Technical Report, Los Alamos Scientific Laboratory*, LA-5852, (1975).
[14] Ozoe H., Toh K., "A Technique to Circumvent a Singularity at a Radial Center with Application for a Three-Dimensional Cylindrical System," *Numerical Heat Transfer B*, 33, pp. 355-365, (1998).
[15] Maki S., Ataka M., Tagawa T., Ozoe H., Mori W., "Natural Convection of a Paramagnetic Liquid Controlled by Magnetization Force," *AIChE Journal*, 51, pp. 1096-1103, (2005).